FFI RAPPORT

ANALYTICAL CAVITY EXPANSION PENETRATION MODELS COMPARED WITH NUMERICAL SIMULATIONS

TELAND Jan Arild, MOXNES John F

FFI/RAPPORT-2003/00934

FFIBM/766/130

Approved
Kjeller 4. March 2003

Bjarne Haugstad
Director of Research

ANALYTICAL CAVITY EXPANSION PENETRATION MODELS COMPARED WITH NUMERICAL SIMULATIONS

TELAND Jan Arild, MOXNES John F

FFI/RAPPORT-2003/00934

FORSVARETS FORSKNINGSINSTITUTT
Norwegian Defence Research Establishment
P O Box 25, NO-2027 Kjeller, Norway

FORSVARETS FORSKNINGSINSTITUTT (FFI)
Norwegian Defence Research Establishment

P O BOX 25
N0-2027 KJELLER, NORWAY

UNCLASSIFIED

SECURITY CLASSIFICATION OF THIS PAGE
(when data entered)

REPORT DOCUMENTATION PAGE

1) PUBL/REPORT NUMBER	2) SECURITY CLASSIFICATION	3) NUMBER OF PAGES
FFI/RAPPORT-2003/00934	UNCLASSIFIED	20
1a) PROJECT REFERENCE	**2a) DECLASSIFICATION/DOWNGRADING SCHEDULE**	
FFIBM/766/130	-	

4) TITLE

ANALYTICAL CAVITY EXPANSION PENETRATION MODELS COMPARED WITH NUMERICAL SIMULATIONS

5) NAMES OF AUTHOR(S) IN FULL (surname first)

TELAND Jan Arild, MOXNES John F

6) DISTRIBUTION STATEMENT

Approved for public release. Distribution unlimited. (Offentlig tilgjengelig)

7) INDEXING TERMS

IN ENGLISH:	IN NORWEGIAN:
a) Cavity expansion theory	a) Hulromsekspansjonsteori
b) Numerical simulation	b) Numerisk simulering
c) Penetration	c) Penetrasjon
d)	d)
e)	e)

THESAURUS REFERENCE:

8) ABSTRACT

Penetration models for rigid projectiles based on cavity expansion theory (CET) are widely used. In this article we performed several hydrocode simulations and compared with analytical results from CET-based theories for the exact same material models. Our aim was to discover whether the complete penetration process was correctly described through the general framework of penetration theories based on CET. It was found that this was generally not the case, although for certain materials the method provided a good estimate of final penetration depth. Improvements that should form part of any new analytical penetration theory were accordingly suggested.

9) DATE	AUTHORIZED BY This page only	POSITION
4. March 2003	Bjarne Haugstad	Director of Research

ISBN-82-464-0754-6

UNCLASSIFIED

SECURITY CLASSIFICATION OF THIS PAGE
(when data entered)

CONTENTS

ANALYTICAL CAVITY EXPANSION PENETRATION MODELS COMPARED WITH NUMERICAL SIMULATIONS

Nomenclature

CET	cavity expansion theory
CETp	cavity expansion theory applied to penetration
σ_r	radial stress on an expanding spherical cavity
σ_r^{stat}	static part of the radial stress on an expanding cavity
σ_r^{dyn}	dynamic part of the radial stress on an expanding cavity
u	radial velocity of an expanding spherical cavity
ρ	density of the target
Y	yield stress of the target
E	Young's modulus of the target
ν	Poisson's ratio of the target
σ_n^p	normal stress on the projectile surface
v	velocity of the projectile
a	radius of the cylindrical projectile
θ	angle between the direction of motion and the normal surface vector of the projectile
A_p	projected area in the direction of motion of the projectile currently in contact with target
l	projectile nose length
c_d	drag coefficient of the projectile
α	half angle of a conical nose

1 INTRODUCTION

Analytical penetration models for rigid projectiles based on cavity expansion theory (CET) are widely used together with simulations and advanced numerical models for describing penetration of rigid projectiles into different materials. The first quasi-static CET model was achieved by Bishop et al [1] during World War II, who constructed a theory for indentation of conical nose punches into ductile materials. In 1960, Hopkins [2] used CET to derive a result for dynamic expansion of spherical cavities in metals. Building on these works, Goodier [3] in 1965 applied CET to the dynamic penetration problem, and thereby was the first to relate CET and penetration mechanics. In this article, CETp will denote penetration theories resulting from use of CET, whereas CET will refer to pure cavity expansion theory only.

The dynamic approach of Goodier was changed by Luk and Forrestal [4] in 1987. They proposed a different relation between the inertial forces and the velocity of the projectile during penetration.

In the last decades, the increase of computer speed and development of hydrocodes has made it possible to perform detailed numerical simulations of the penetration process. Three different approaches are used by most advanced penetration groups; i) highly analytical models, ii) simplified numerical models, iii) hydrocode simulations. By appealing to different types of approaches during penetration studies, a better understanding of the main physical mechanisms have been achieved.

The accuracy of the computer simulations and some material models was tested by Børvik et. al. [5] by comparing 24 different high–precision large scale impact test with numerical results from hydrocode simulations. In general, close correlation between numerical and experimental results was achieved for the different targets and nose shapes.

However, full 3D-simulations still require excessive CPU-time and are therefore impractical for performing parameter and sensitivity studies. Hybrid simulations [6-8], where some of the time-consuming numerical processes are replaced by analytical theory, is one way to significantly decrease the runtime. It is clear that the value of such simulations is strongly dependent on the accuracy of the analytical method.

At high impact velocities where hydrodynamic forces are comparable with quasi-static mechanical forces, CETp can usually not be applied because the projectile deforms upon impact with the target. In these cases more hydrodynamic theories for the flow of the projectile have to be used [9-12]. In recent years, after the Gulf war, focus has shifted towards penetration into “soft” targets as concrete and various building materials. When considering for instance a wolfram-carbide penetrator with a velocity of 1500 m/s, even concrete may be considered a soft material, but hydrodynamic forces might still play a very important role.

In this paper we perform several numerical simulations and compare with analytical results for the exact same material models. We discover that in general the force on the projectile as a function of time is not correctly described through the framework of CETp. However, the discrepancies in some cases have a tendency to cancel out when integrated over the complete penetration process, leading to a good estimate of the final penetration depth. Improvements that should be a part of an improved analytical penetration theory are accordingly suggested.

2 CAVITY EXPANSION THEORY

CET deals with the problem of finding the radial stress required to expand a cavity inside a given material. Traditionally, spherical and cylindrical cavities have been considered, giving rise to both spherical and cylindrical CET. In this article we will focus on spherical CET since this model is most commonly used.

Assuming the spherical cavity to be expanding at velocity u in an infinite Mises material, the required radial stress can be divided into static and dynamic parts [13]:

$$\sigma_r = \sigma_r^{stat} + \sigma_r^{dyn},$$
$$\sigma_r^{stat} = \frac{2Y}{3}\left(1 + ln\left(\frac{E}{3(1-\upsilon)Y}\right)\right), \tag{2.1}$$
$$\sigma_r^{dyn} = \left(\frac{3}{2}\right)\rho\, u^2,$$

Observe that the contributions from the material strength (static part) and the inertia (dynamic part) are additive.

3 CAVITY EXPANSION THEORY APPLIED TO PENETRATION

The process of expanding a cavity in a given material is somewhat similar to the process where a rigid projectile penetrates into that material. As a consequence, CET has often been applied to penetration problems.

For a rigid projectile moving in the x-direction, the total force can always be found by integrating the stresses over the projectile body. It is convenient to write the total force in the following way:

$$F = \int_{A_p} \sigma_n^p(x)\, dA_p(x) \tag{3.1}$$

where σ_n^p is the normal stress on the projectile and $A_p(x)$ is the projected surface area along the direction of motion which is currently in contact with the target. To relate CET to penetration, we need to find a relationship between the actual normal stress σ_n^p on a projectile penetrating at velocity *v,* and the radial stress σ_r from CET of a cavity expanding at a velocity *u*.

Goodier [3] proposed that; a) the radial stress from CET should be used as the normal stress on the projectile body and; b) the inertial stress from CET should be projected along the axis of motion of the projectile. The more specific relation using (3.1) is

$$\sigma_n^p = \sigma_r^{stat} + \sigma_r^{dyn}(v)\cos\theta = \sigma_r^{stat} + \frac{3}{2}\rho v^2 \cos\theta \tag{3.2}$$

The dynamic part of this relation was much later changed by Luk and Forrestal [4], who instead assumed the relation between the expansion velocity *u* from CET and the penetration velocity *v* to be given by $u = v\cos\theta$. This leads to the following expression, which today is generally accepted:

$$\sigma_n^p = \sigma_r^{stat} + \sigma_r^{dyn}(v\cos\theta) = \sigma_r^{stat} + \frac{3}{2}\rho v^2 \cos^2\theta \tag{3.3}$$

However, as we shall see, it has to be changed to adequately describe the penetration process.

3.1 Spherical nose

For the special case of a projectile with a spherical nose projectile, we have:

$$A_p(x) = \begin{cases} \pi a^2 \left(2x/a - x^2/a^2\right) & x \le a \\ \pi a^2 & x \ge a \end{cases} \tag{3.4}$$

The force on penetrator according to Goodier's approach in Equation (3.2), is then given by:

$$F = \int_{A_p} \sigma_n^p dA_p = \left(\sigma_r^{stat} + \frac{1}{2} c_d(x) \rho v^2\right) A_p(x),$$
$$c_d(x) = \begin{cases} \left(\dfrac{2(3 - x/a)}{(2 - x/a)}\right) - 2x/a & x \le a \\ 2 & x \ge a \end{cases} \tag{3.5}$$

where $c_d(x)$ is the so-called drag coefficient, defined in accordance with fluid dynamics [14].

Using the generally accepted method of Equation (3.3) gives us a similar expression for the force, but with a different drag coefficient:

$$c_d(x) = \begin{cases} \dfrac{3}{2}\left(1 + (1 - x/a)^2\right) & x \le a \\ \dfrac{3}{2} & x \ge a \end{cases} \tag{3.6}$$

3.2 Conical nose

For a projectile with conical nose of half angle $0 < \alpha < \pi/2$, we have:

$$A_p(x) = \begin{cases} \pi x^2 \tan^2 \alpha & x \le a/\tan\alpha \\ \pi a^2 & x \ge a/\tan\alpha \end{cases} \tag{3.7}$$

On using Goodier's method, the force obeys the same expression as in Equation (3.5), except for a different drag coefficient:

$$c_d = 3\cos\alpha \tag{3.8}$$

The generally accepted method of Equation (3.3) gives another expression for the drag coefficient:

$$c_d = 3\cos^2\alpha \tag{3.9}$$

We note that the expression for the force takes on the same form in each case, except for the drag coefficient which is strongly dependent on the projectile nose geometry. For the spherical

nose it decreases as the projectile enters the target, whereas the conical nose gives a constant drag coefficient. In our analysis we will use the drag coefficients obtained from Equation (3.3).

It is clear that the penetration process can be conveniently divided into two phases. The first (cratering) phase is characterized by the projectile nose not having completely entered the target, whereas in the second (tunneling) phase, the nose is completely embedded.

Now that an expression for the force has been found, and the projectile is assumed rigid, the complete penetration process can easily be calculated using Newton's 2nd law.

4 SIMULATIONS

Using Autodyn-2D we performed simulations to investigate the predictions of the analytical model with the "correct" numerical results for the same problem. Our aim was to discover whether the complete penetration process (force on the projectile) was correctly described through the general framework of CETp. It is emphasized that we are investigating CETp, i.e. CET applied to penetration and not CET itself, which is an exact theory.

We will look at two different projectile geometries (spherical and conical nose) impacting against both hard and soft target materials. Very simple elastic-plastic material models were deliberately chosen so that our study could be carried out with exactly the same materials analytically and numerically.

The two projectile geometries are depicted in Figure 4.1. The radius was 7.5 cm and the masses were 28.17 kg and 32.03 kg for the spherical and conical nose projectile, respectively.

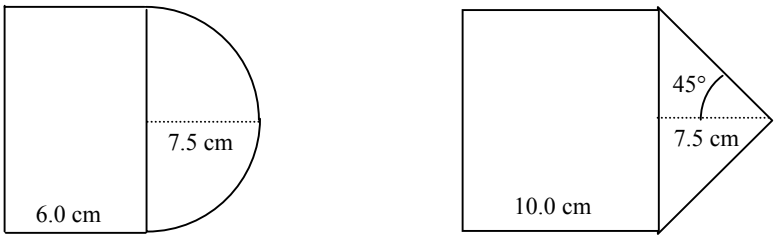

Figure 4.1 : Projectile geometries.

The cylindrical steel targets had a diameter of 153 cm and a length of 143 cm. The concrete targets had a diameter of 153 cm and a length of 286 cm. The value of the various material parameters are given in Table 4.1.

Table 4.1: Values of the various material parameters.

	Wolfram carbide	Steel	Concrete
Density (g/cm^3)	14.50	7.84	2.00
Bulk modulus (GPa)	210.92	171.67	79.23
Shear modulus (GPa)	151.65	5.33	4.00
Yield limit (MPa)	-	1100	250

It is an assumption of CETp that the projectile behaves rigidly during the whole penetration process. However, on using the regular elastic parameters for wolfram there turned out to be huge oscillations in the force on the projectile as a function of time. The reason was found to be elastic oscillations of the projectile due to the finite E-modulus. By increasing the E-modulus with a factor of 10, the amplitude of the oscillations were significantly reduced. We also experimented with values up to 1000 times the original, but this did not lead to a significant improvement in the results. As a compromise between runtime and accuracy, a factor of 10 times the original E-modulus was therefore used in the simulations.

5 RESULTS FOR SPHERICAL NOSE

Here we present the results for impact of the projectile with spherical nose against hard and soft targets, respectively. The penetration depth was found by integrating the velocity of the centre of mass of the penetrator. The force was similarly obtained by differentiating the velocity of the centre of mass.

5.1 Hard target

In Figure 5.1 we have plotted the simulated force as a function of penetration depth for an impact velocity of 1500 m/s, together with the solutions from the static and dynamic spherical CETp.

The dynamic CETp force is close to the Autodyn force during the first part of the cratering phase. However, when the nose is almost halfway into the target, the Autodyn force suddenly declines rapidly and reaches static CETp at the start of the tunnelling phase. This indicates that the static part of the CETp remains a good approximation during the whole penetration process, whereas the dynamic part only gives a good description very early in the process. In fact, the simulations seems to indicate that the dynamic contribution should be almost negligible during the tunnelling phase.

Figure 5.2 shows the analogous curves for an impact velocity of 500 m/s. The same tendency as for the 1500 m/s impact is observed, i.e. that dynamic CETp is very close to the simulation result initially, but then overpredicts the force.

Interestingly, we also notice that the Autodyn force is lower than what is found from static CETp. This effect was also present for the 1500 m/s impact, but not so clearly visible as in Figure 5.2. The deficit compared with the static CETp indicates that also the analytical static term should be slightly modified. A closer examination showed that the cylindrical CETp is closer to the simulated values for lower velocities in this case.

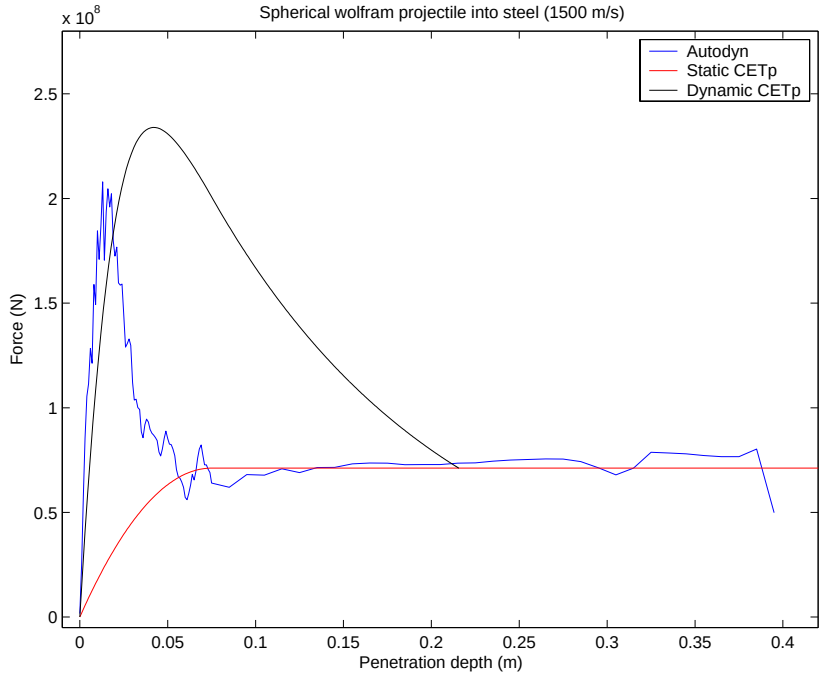

Figure 5.1: Force as a function penetration depth for impact against steel at 1500 m/s.

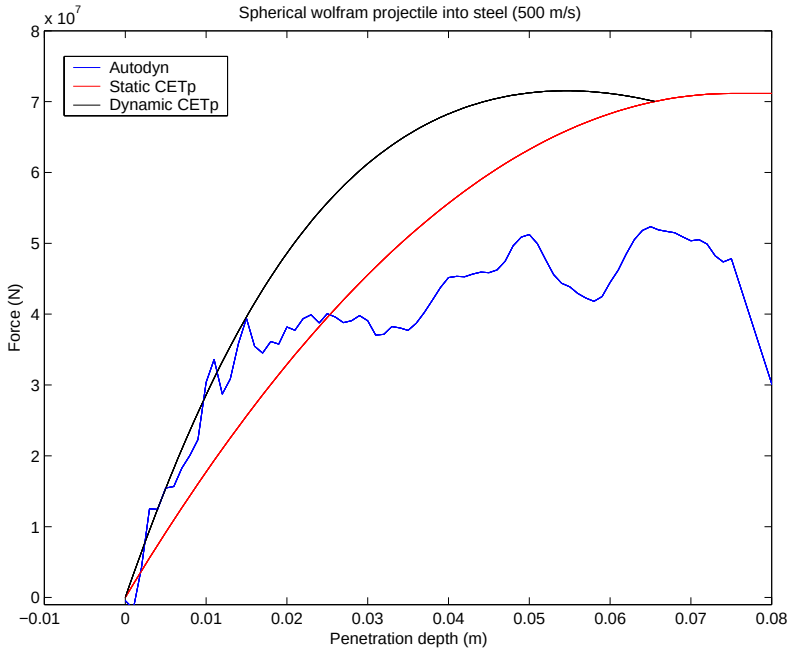

Figure 5.2: Force as a function of penetration depth for impact against steel at 500 m/s.

5.2 Soft target

We now turn our attention to impact on a relatively soft target. As an example we have used material model roughly corresponding to concrete (see Table 4.1). In general, concrete requires a much more complicated material model than the perfect elastic plastic model which is considered here. However, the main point of this study was to compare the analytical CETp with simulations for exactly the same material models. Applying the most advanced concrete models would only have served to confuse the situation.

Figure 5.3 is analogous to Figure 5.1. We observe once again that dynamic CETp is a very good approximation in the initial part of the cratering phase, but then strongly overpredicts the force in the tunneling phase.

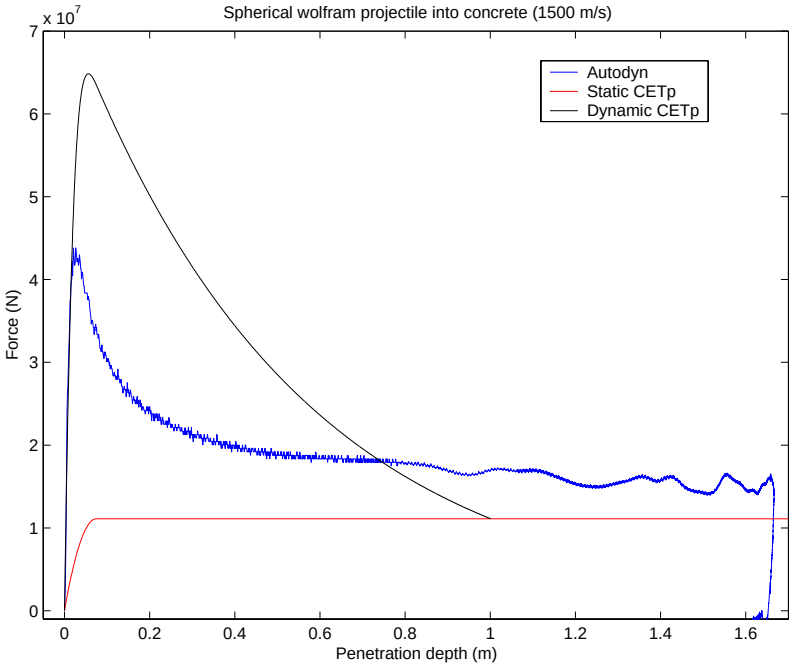

Figure 5.3: Force as a function of penetration depth for impact against concrete at 1500 m/s.

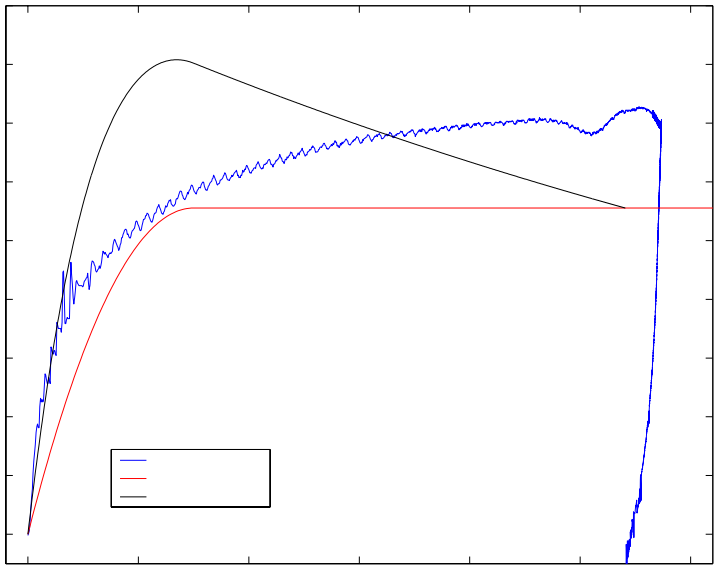

Figure 5.4: Force as a function of penetration depth for impact against concrete at 500 m/s

Figure 5.4 is analogous to Figure 5.2. On examining this plot, we notice that the simulated force increases during the tunnelling phase when the projectile velocity decreases. Intuitively, this is difficult to understand. CETp fails to explain this phenomenon, which is probably connected with dynamic effects not accounted for in the analytical theory.

We also observe that the simulated force is (asymptotically) larger than the force from static static CETp. This effect is the opposite of what we observed for the steel target, and therefore suggests that the use of cylindrical CETp instead of the spherical CETp expansion is not an appropriate solution.

Since the force is overpredicted early in the penetration process and underpredicted late in the process, we note that these two effects almost cancel each other out, leading to good agreement for the final penetration depth for this case.

6 RESULTS FOR CONICAL NOSE

In this chapter we review the results from similar simulations with a conical nosed projectile.

6.1 Hard target

Figure 6.1 is analogous to Figure 5.1 and depicts the force as a function of penetration depth for an impact velocity of 1500 m/s. The results show exactly the same tendency as for the spherical projectile. The simulated force follows dynamic CETp initially in the cratering phase and then declines rapidly to almost reach static CETp during the tunnelling phase.

Figure 6.2 shows the same situation as in Figure 5.2. Again the simulated force is somewhat smaller than the static force calculated from CETp.

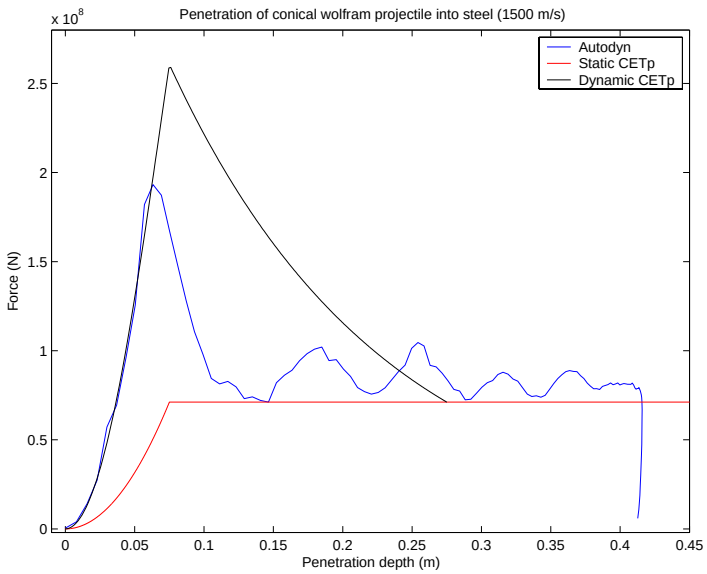

Figure 6.1: Force-penetration depth for a conical nose impacting steel at 1500 m/s.

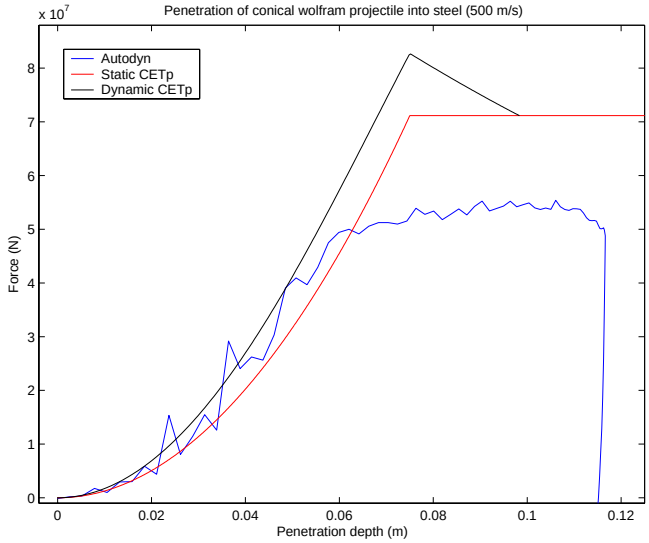

Figure 6.2: Force-penetration depth for a conical nose impacting steel at 500 m/s.

6.2 Soft target

The results for the conical nose projectile against the soft targets are illustrated in Figures 6.3 and 6.4.

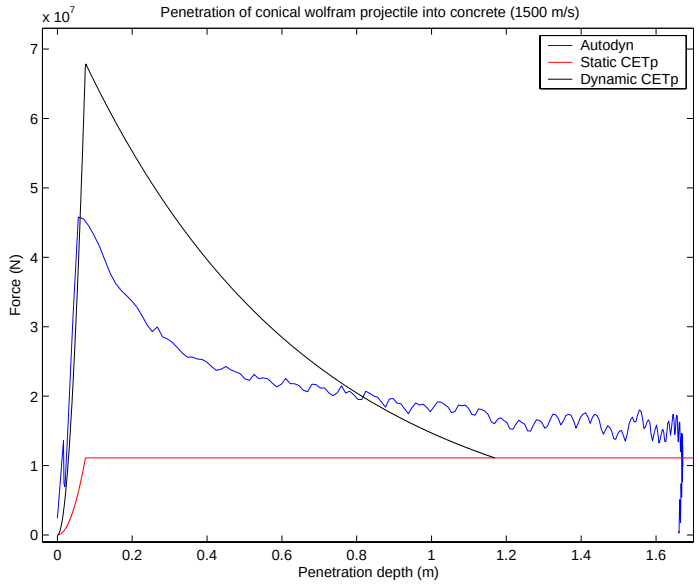

Figure 6.3: Force-penetration depth for a conical nose impacting a soft target at 1500 m/s.

Both simulations show the same tendency compared with analytical CETp, as was observed for the spherical nosed projectile. From Figure 6.3 the dynamic contribution in CETp is again seen to overestimate the simulated force, whereas Figure 6.4 gives the same tendency as in Figure 5.4 showing once more the deficit of static CETp.

Again we note that the overprediction of the force early in the process seems to cancel out the underprediction later on, leading to excellent agreement between dynamic CETp and Autodyn for final penetration depth.

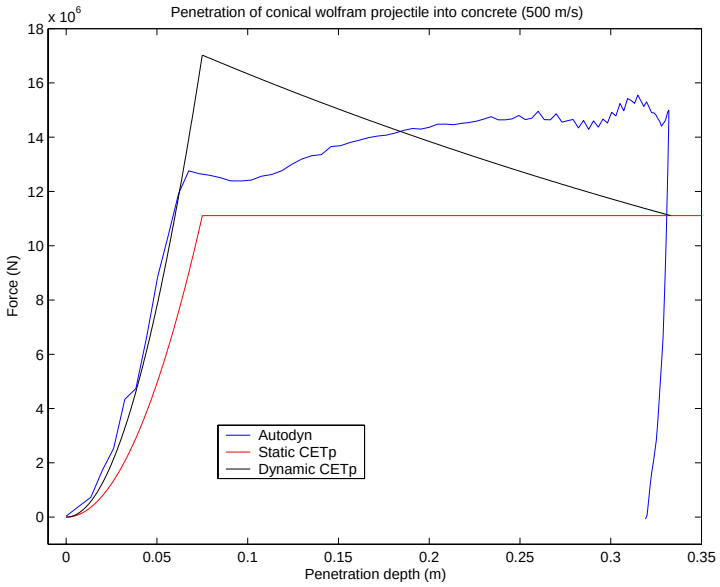

Figure 6.4: Force-penetration depth for a conical nose impacting a soft target at 500 m/s.

We also once more observe the mysterious phenomenon that the force increases with penetration depth in the tunnelling phase. There is a kink in the Autodyn force-curve at the depth where the nose is embedded, after which the force briefly starts decreasing. So far everything is as expected since the velocity decreases with penetration depth and the dynamic contribution to the force should therefore decrease.

However, instead of continuing to decline towards the static CETp value, the Autodyn force suddenly starts increasing again, as Figure 6.4 so clearly shows. By analysing the numerical simulations more closely we have found that the phenomenon is not related to boundary effects of the target. The results could be related to numerical artefacts in the hydrocode, but the following hypothesis is advanced:

According to Equation (2.1) of CETp, the inertial forces and mechanical forces are additive and the mechanical strength term is independent of the velocity. We believe that this is not valid in general. In [15] the drag coefficients and slip angles[1] for impact of steel spheres into very weak soap targets was analysed both numerically and experimentally. It was found that the slip angle could be as low as $\pi/4$ at high velocities. This observation is important since it suggests that the mechanical strength term could be decreasing with velocity.

If the slip angle decreases at high velocities, the contribution from the mechanical strength term must also decrease since integration of the stress should only be carried out over the relevant part of the projectile nose surface, i.e. where the nose is in contact with the target material. This introduces a velocity dependence into the the mechanical strength term, which is then seen to be decreasing with velocity. Since the inertial term increases with velocity and the mechanical strength decreases, there are two competing effects which in some cases may lead to a local maximum for the total force at a specific velocity. We believe that this effect explains the observations in Figure 6.4.

[1] The slip angle is the angle where the projectile nose is no longer in contact with the target material.

This phenomenon further opens for a scenario where for some targets and some velocities, increasing the initial velocity of the penetrator leads to a decreasing force on the penetrator and thereby to a surprisingly large increase in the penetration depth.

We have so far not observed the above described phenomenon for hard targets as steel. This is probably because a large mechanical term means that the target material is not so easily thrown away from the nose and the slip angle therefore always remains close to $\pi/2$. Consequently, the mechanical term is only weakly dependent on velocity and the inertial term dominates so that no local maximum is observed.

7 CONCLUSIONS

We have observed that that the dynamic CETp expression is in good agreement with Autodyn in the early stage of the penetration phase where the projectile enters the target. This lasts until the projectile nose is about halfway into the target when suddenly the curves diverge. That dynamic CETp is so accurate initially in the cratering phase is probably due to this phase being similar to cavity expansion, unlike the tunnelling phase of the penetration process.

Also the simulated force in a soft target continues increasing with the current penetration depth for an initial velocity of 500 m/s, even after the projectile nose is completely embedded in the target. This is unexpected since the projectile slows down as it enters the target, which should lead to smaller inertia. This phenomenon is not accounted for in CETp, but we suggest that it is related to increase in the mechanical strength term with decreasing velocity.

A new analytical theory has not yet been created. However, it is suggested that by using spherical dynamic CETp models for the first part of the cratering phase and a hydrodynamic theory with a decreased drag coefficient for the tunnelling phase, much better agreement for the force as a function of penetration depth is possible to achieve. The simulations also indicate that the static CETp term should be somewhat corrected for small velocities.
We suggest that more research is needed on the following topics:

- Prove mathematically that the dynamic spherical CETp theory is a good approximation in the first phase.

- Prove mathematically that the hydrodynamic theory with reduced or corrected drag coefficient, is a good approximation for the tunnelling phase. Also derive the “cut-off” point where the two theories merge.

References

[1] Bishop R F, Hill R, Mott N F, The theory of indentation and hardness, *Proc. Roy. Soc.* **57,** Part 3, 147-159 (1945)

[2] Hopkins H G, Dynamic expansion of spherical cavities in metals, *Progress in Solid Mechanics,* Vol. 1, Chapter III, North-Holland Publ. Co., Amsterdam, New York (1960)

[3] Goodier J N, On the mechanics of indentation and cratering in solid targets of strain-hardening metal by impact of hard and soft spheres, *Proc. 7th Symposium on Hypervelocity Impact III,* pp. 215-259. AIAA, New York (1965)

[4] Luk V K, Forrestal M J, Penetration into semi-infinite reinforced concrete targets with spherical and ogival nose projectiles, Int J Impact Engng Vol. 6, No. 4, pp. 291-301 (1987)

[5] Børvik T, Langseth M, Hopperstad O S, Malo K A, Perforation of 12mm thick plates by 20 mm diameter projectiles with flat, hemispherical and conical noses, Part I and Part II, *Int J Impact Engng,* Vol. 27, pp. 19-64 (2002)

[6] Warren T L, Poormon K L, Penetration of 6061-T6511 aluminium targets by ogive-nosed VAR 4340 steel projectiles at oblique angles: experiments and simulations, *Int J Impact Eng,* Vol. 25, pp. 993-1022 (2001)

[7] Olsen Å A F, Teland J A, Rapid numerical 3D penetration simulations using a virtual target, FFI/RAPPORT-2002/00575

[8] Teland J A, Examination of yawed impact using a combined analytical and numerical method, Proceedings 11th Int Symposium on the Interaction of Munitions with Structures (2003)

[9] Birkhoff G, MacDougall D P, Pugh E M, Taylor G, Explosives with lined cavities, J. Applied Physics, Vol.19, No.6, pp. 563-582 (1948)

[10] Alekseevskii V P, Fizika Goreniya i Vzryva, Vol.2, No.2, pp. 99-106 (1966)

[11] Tate A, A theory for the deceleration of a rod into a target at high velocity, J. Mech. Phys. Solids Vol.15, pp. 387-399 (1967)

[12] Walker J D, Anderson C E, A time-dependent model for long-rod penetration, Int. J. Impact Engng Vol.16, No.1, pp. 19-48 (1995)

[13] Teland J A, A review of analytical penetration theory, FFI/RAPPORT-99/01264

[14] Landau L D, Lifshitz E M, Fluid Mechanics, pp.145-182 (1982)

[15] Martinussen S E, Moxnes J F, Cavity expansion theory applied to the penetration of high speed spheres into weak targets, FFI/RAPPORT-2002/03291

DISTRIBUTION LIST

FFIBM **Dato:** 4. mars 2003

RAPPORTTYPE (KRYSS AV)	RAPPORT NR.	REFERANSE	RAPPORTENS DATO
X RAPP ☐ NOTAT ☐ RR	2003/00934	FFIBM/766/130	4. mars 2003
RAPPORTENS BESKYTTELSESGRAD		ANTALL TRYKTE UTSTEDT	ANTALL SIDER
Unclassified		18	20
RAPPORTENS TITTEL		FORFATTER(E)	
ANALYTICAL CAVITY EXPANSION PENETRATION MODELS COMPARED WITH NUMERICAL SIMULATIONS		TELAND Jan Arild, MOXNES John F	
FORDELING GODKJENT AV FORSKNINGSSJEF		FORDELING GODKJENT AV AVDELINGSSJEF:	
Bjarne Haugstad		Jan Ivar Botnan	

EKSTERN FORDELING

ANTALL	EKS NR	TIL

INTERN FORDELING

ANTALL	EKS NR	TIL
9		FFI-Bibl
1		FFI-ledelse
1		FFIE
1		FFISYS
1		FFIBM
1		FFIN
4		Forfattereksemplar(er)
		Restopplag til Biblioteket
		Elektronisk fordeling:
		FFI-veven
		Bjarne Haugstad (BjH)
		Svein Rollvik (SRo)
		Eirik Svinsås (ESv)
		Henrik Sjøl (HSj)
		Knut B Holm (KBH)
		Svein E Martinussen (SEM)

Benytt ny side om nødvendig.